

Dielectric switching of the nature of excited singlet state in a donor-acceptor-type polyfluorene copolymer

Annamaria Petrozza,^{1,2} Frédéric Laquai,^{1,4} Ian A. Howard,^{1,4} Ji-Seon Kim,^{3,*} and Richard H. Friend¹

¹*Cavendish Laboratory, University of Cambridge, J.J. Thomson Avenue, Cambridge CB3 0HE, United Kingdom*

²*Center for Nano Science and Technology of IIT@PoliMI, Via Pascoli 70/3 20133 Milano, Italy*

³*Blackett Laboratory, Imperial College London, Prince Consort Road, London SW7 2AZ, United Kingdom*

⁴*Max Planck Research Group for Organic Optoelectronics, Max Planck Institute for Polymer Research, Ackermannweg 10, D-55128 Mainz, Germany*

(Received 20 January 2010; published 12 May 2010)

The spectral evolution of an intrachain neutral singlet exciton toward a charge-transfer (CT) state in solvents of increasing polarity has been monitored by time-resolved photoluminescence and ultrafast transient-absorption spectroscopy in a model conjugated random copolymer composed of electron donor and electron acceptor units. In polar solvents, a charge-like absorption superimposes the region of stimulated emission and leads to a dramatic reduction in gain implying that CT states can be detrimental for light amplification and lasing.

DOI: 10.1103/PhysRevB.81.205421

PACS number(s): 82.30.Fi, 61.25.hk, 71.35.Cc, 73.20.Mf

I. INTRODUCTION

Charge-carrier generation in blends of donor- and acceptor-type conjugated materials has attracted much interest during the past decade due to the potential use of such systems in bulk heterojunction organic photovoltaic devices. Phase separation on the nanometer scale (commensurate with exciton diffusion length) is a prerequisite for the primary photoexcitation to reach the heterojunction where an intermolecular charge-transfer (CT) state is formed.¹ The use of copolymerisation to generate electron donor-acceptor- (D-A-) type interactions has recently attracted much interest since this not only allows control of the nanostructure formation but also creates unique optoelectronic properties, which contribute to the formation of interchain and intrachain CT states.

The intrachain CT state exhibits typically a significant emission wavelength dependence on the polarity of the local environment due to its strong dipolar character. Hence, pronounced solvatochromism can typically be observed with increasing solvent polarity. Experimental results on conjugated small molecules suggest that in case of a Marcus-type nonadiabatic electron-transfer process, these systems exhibit a dynamic equilibrium between a locally excited (LE) singlet state and the CT state, whose equilibrium position depends on the solvent-induced stabilization of the CT state and the temperature of the system.² To date, there have only been a few reports on the photophysical properties of intrachain CT states in conjugated polymers,³⁻⁵ despite CT states being well known in conjugated small molecules.

Here, we report on the photophysical properties of intrachain CT states formed after excitation in a random copolymer (RC) consisting of 9,9'-di-*n*-octylfluorene-*alt*-*N*-(4-butylphenyl)diphenylamine, TFB (electron donor) and 9,9'-di-*n*-octylfluorene-*alt*-benzothiadiazole, F8BT (electron acceptor) units (Fig. 1). We have monitored a distinctive spectral evolution of the excited state in RC chains in solution by using ultrafast transient-absorption (TA) and time-resolved photoluminescence (PL) spectroscopy techniques.^{6,7} Our results highlight

a dielectric controlled switching from a tightly bound neutral singlet exciton toward an intrachain CT state that further exhibits pronounced charge-like photoinduced absorption features.

II. EXPERIMENTAL METHODS

The conjugated polymers, F8BT ($M_n=9$ Kg/mol) and RC ($M_n=40$ Kg/mol) were received from CDT Ltd. and used as received. The RC was synthesized by Suzuki cross-coupling reaction between the boronic ester of 9,9'-dioctylfluorene (F8), dibromide-benzothiadiazole (BT),

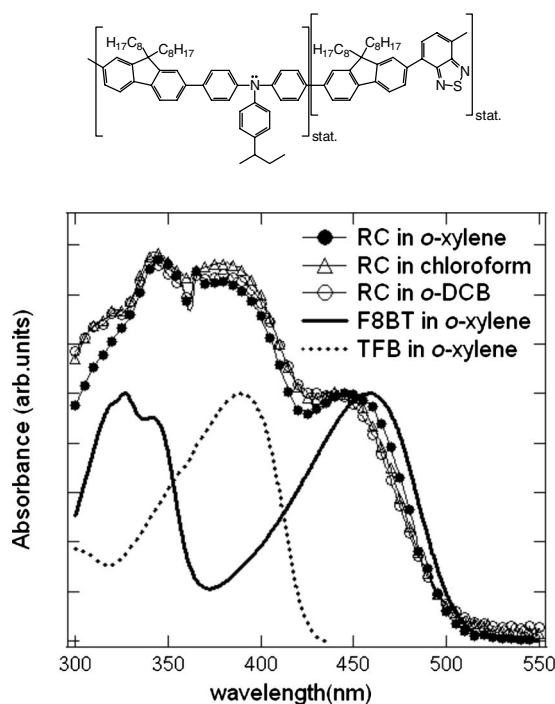


FIG. 1. UV-Vis absorption spectra of RC diluted in solvents of increasing polarity: *o*-xylene, chloroform, and *o*-DCB. F8BT and TFB absorption spectra in dilute *o*-xylene solutions are also shown. The chemical structure of RC is shown on top of the figure.

and dibromide-triarylamine monomers. Hence, the two latter monomers are always covalently linked to one fluorene unit during the cross-coupling reaction. The polymer solutions were prepared in a concentration of $0.1-10^{-6}$ % (*w/v*). The RC showed very good solubility in all solvents, except for the cyclohexane solution, which was heated to 75 °C and measured immediately.

Absorption spectra were taken using a Hewlett Packard 8453 UV-Vis spectrometer. The solvent absorption spectrum was taken as reference. Time-integrated photoluminescence spectra were acquired by an Acton Research 2500i spectrometer coupled to a PIMAX100 charge-coupled-device array using pulsed (40 MHz, 800 ps full width at half maximum, FWHM, 470 nm) diode laser (PicoQuant LDH400) for excitation. Solution samples were measured in spectroscopic grade cuvettes in an oxygen-free atmosphere. The temperature-dependent measurements were performed using a chiller connected to a temperature-controlled sample holder.

Time-correlated single-photon counting (TCSPC) was performed to measure fluorescence lifetimes in the time window between 1 and 200 ns. Samples were excited with a pulsed (300 ps FWHM, 470 nm) diode laser (PicoQuant LDH400). The luminescence was detected with a microchannel plate photomultiplier (Hamamatsu) coupled to a spectrometer and TCSPC electronics (Edinburgh Instruments Lifespec-ps and VTC900 PCI card).

TA spectroscopy was used to study the evolution and dynamics of the excited states on a time scale of hundreds of femtoseconds to milliseconds by probing the relative change in transmission ($\Delta T/T$) after photoexcitation. Samples were typically excited at 490 nm using the output of a traveling-wave optical parametric amplifier of superfluorescence (TOPAS) system (Light Conversion) pumped by a Ti:sapphire amplifier system (Spectra-Physics Tsunami combined with Spitfire) with a typical pulse duration of ~ 100 fs and a repetition rate of 1 kHz. The excitation power was varied between 40 and 250 μ W by neutral density filters. A linear dependence of the photoinduced absorption signal on the excitation power was verified, therefore the excitation power was adjusted to get a reasonable signal-to-noise ratio of the photoinduced absorption signal.

The transient-absorption characteristics were probed with a white-light continuum, derived from a home-built noncollinear optical parametric amplifier (NOPA) similar to the one described in Ref. 7. The NOPA generates an amplified white-light continuum typically in the range of 500–800 nm according to the broadband phase matching achieved in the crystal. A white-light seed was generated by focusing a fraction (about 2–3 μ J) of the output of the regenerative amplifier into a 2 mm sapphire plate and the white light was then amplified in the beta barium borate (BBO), non-collinear optical parameter amplifier (NOPA) crystal (cut at 32°) by overlapping the seed with a 400 nm pump (about 60 μ J) under a noncollinear angle of approximately 3.8°. Only reflective optics were used to focus and collimate the white-light seed and the NOPA output to keep the chirp of the white-light probe as little as possible without further compression. Both beams, the femtosecond pump and white-light probe were focused onto the sample surface. Optimal spatial

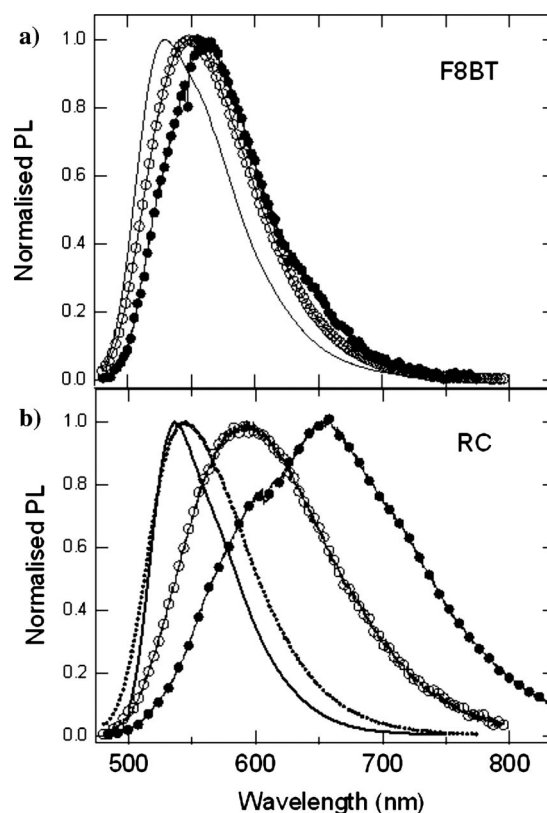


FIG. 2. PL spectra of diluted solutions of (a) F8BT and (b) RC in solvents with increasing polarity, cyclohexane (solid line), *o*-xylene (dot line), chloroform (empty circles), *o*-DCB (filled circles). Excitation at 470 nm.

overlap was guaranteed by ensuring a significantly smaller probe beam spot (generally about 400 μ m at FWHM). The probe beam arrival was varied in time relative to the pump pulse arrival by a mechanical delay stage.

III. RESULTS

The RC has a strong intrinsic intrachain D-A character, i.e., the highest occupied molecular orbital (HOMO) lies mainly on the triarylamine unit and the lowest unoccupied molecular orbital (LUMO) is strongly localized on the BT unit.⁸ In spite of this strong D-A character, the RC does not exhibit any additional ground-state absorption features compared to the neat F8BT and TFB polymers, in fact the absorption spectrum can be modeled as the superposition of the absorption spectra of F8BT and TFB single components (Fig. 1).⁸ The absence of any direct transitions to the CT state may result from the very weak transition strength due to well-separated “hole” and “electron” that comprise the CT state. As is also the case for F8BT, the absorption spectrum of the RC did not exhibit any distinct solvent dependence. Such dipolar solvent-independent absorption spectra in the RC may indicate that the unrelaxed excited state reached immediately after absorption is not strongly associated with a significant permanent dipole moment, irrespective of any intrachain CT character present within the RC D-A units.

The luminescence behavior however is very different. The solvent-dependent PL spectra of F8BT and RC in solutions

TABLE I. Properties of solvents and summary of the fluorescence position and lifetime of RC solutions.

Solvent	Viscosity at 25 °C (mPa s)	Dielectric constant	PL peak (nm)	Lifetime (ns)
Cyclohexane	0.894	2.02	536	
<i>o</i> -xylene	0.760	2.57	545	2.6
Chloroform	0.537	4.81	587	5.2
<i>o</i> -DCB	1.324	9.93	650	5.7

of increasing polarity are shown in Figs. 2(a) and 2(b), and summarized in Table I. F8BT showed a redshift of ~ 30 nm of its fluorescence maximum, when the solvent polarity was increased from *o*-xylene to *o*-dichlorobenzene (*o*-DCB), indicating the polar nature of its relaxed emissive state. The solvatochromic effect in RC is considerably stronger. The fluorescence peak was found to redshift from 536 to 587 nm accompanied by considerable spectral broadening as the solvent polarity was increased from nonpolar (cyclohexane) to polar (chloroform). The fluorescence lifetime of RC was found to be longer compared to F8BT in *o*-xylene solutions (2.6 ns vs 2.0 ns), with a further increase to 5.2 ns in chloroform solution. The fluorescence decay traces (not shown) were well fitted by a monoexponential decay over the entire spectral range indicating the presence of a single emissive species. Increasing the solvent polarity even further (to *o*-dichlorobenzene) caused the main fluorescence peak to redshift to 650 nm and its lifetime to increase to 5.7 ns, however, still showing a monoexponential profile. Interestingly, a shoulder emerged in the PL spectrum at 590 nm, which is close to the spectral position of the maximum of the F8BT fluorescence. A double exponential decay profile was found in this spectral range.

The effect of solvent polarity on the emission shift can be utilized to infer the degree of intrachain charge transfer in the relaxed excited state. The dependence of the energy of a molecular state upon polarizability and polarity of the solvent can be well rationalized with standard equations including the dipole moment of the state, i.e., the effect of solvent polarity on the emission shift can be utilized to infer the degree of intrachain charge transfer in the relaxed excited state. For steady-state emission spectra where solvent relaxation has already reached its equilibrium arrangement around the solute, the Stoke shift ($E_a - E_f$) of a solute in a solvent with static dielectric constant ϵ and refractive index n can be estimated based on the macroscopic dielectric theory,^{9,10}

$$E_a - E_f = \frac{2(\mu_e - \mu_g)^2}{a^3} \left[\frac{\epsilon - 1}{\epsilon + 1} - \frac{n^2 - 1}{n^2 + 2} \right],$$

where μ_g and μ_e are the ground-state and excited-state permanent dipole moment, respectively, and a is the interaction cavity radius (Onsager interaction radius). From the above expression, the permanent dipole moment change upon photoemission, $\Delta\mu = (\mu_e - \mu_g)$, of the RC can be determined from the slope of the solvatochromic plot (Fig. 3) if the value of a is known. If one assumes the cavity radius a to be the spherical volume of the bulkiest TFB unit in the RC

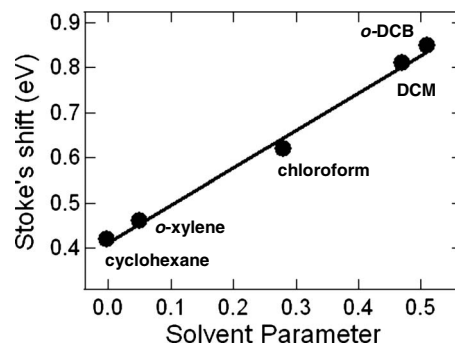


FIG. 3. The solvatochromic plot—the Stoke shift of the RC in different solvents with varying solvent parameter. The slope of the plot indicates the degree of intramolecular charge transfer in the excited state.

(~ 5 Å) and the relatively small ground-state dipole moment compared to the excited-state dipole moment ($\mu_e \approx 0$), we can obtain $\Delta\mu \sim 7$ D. This value, however, needs to be taken with care as the size of the chromophore and its relation to the cavity radius are still an issue of debate for conjugated polymers.

The observed sensitivity of the emissive state to the solvent polarity strongly supports its CT character in the relaxed geometry.¹⁰ Note that distinguishing the effect induced by ionic interaction from that induced by conformational changes in the molecule on the dynamical shift in the RC emission is not trivial. The principal geometrical factor that affects excited-state energies in the RC is the torsion angle between the BT and adjacent F8 groups, and in general this is reduced (toward planarity) in the excited state, and will therefore contribute to a dynamical redshift in emission.⁸

The TA spectra of F8BT in diluted *o*-xylene solution [Fig. 4(a)] present two main features. For wavelengths (λ) < 600 nm, a positive differential transmission signal ($\Delta T/T$) was observed. It is assigned to stimulated emission (SE) originating from the first excited singlet state since its spec-

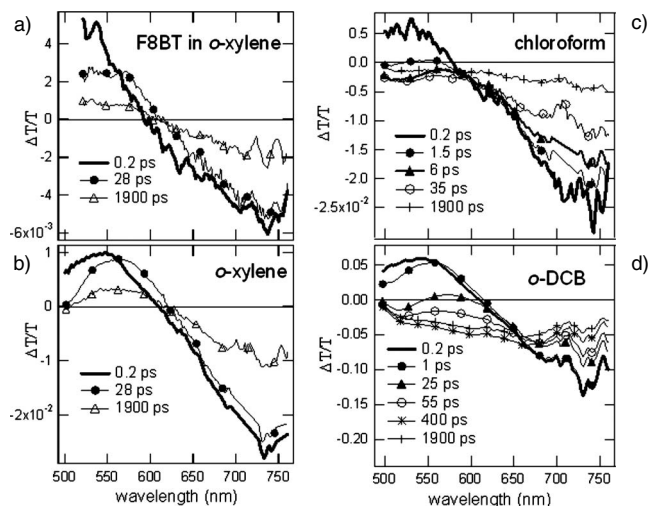


FIG. 4. Femtosecond to picosecond transient-absorption spectra of (a) F8BT in *o*-xylene solution and RC in (b) *o*-xylene, (c) chloroform, and (d) *o*-DCB solutions. Excitation at 490 nm.

tral position matches the fluorescence of the polymer. The SE could be observed over the entire detection time (about 2 ns). At $\lambda > 600$ nm, a photoinduced absorption (PA) band occurred which extended into the near infrared. This arises from the $S_1 \rightarrow S_n$ excited-state absorption since the SE and PA bands exhibited the same lifetimes and decay dynamics.¹¹ A spectral broadening of the SE band was observed for *o*-xylene solution whereas in the polar solvents (chloroform and *o*-DCB), a distinct dynamic redshift of the band was observed (not shown). This is in agreement with the solvatochromic effect observed in the steady-state PL spectra and confirms the presence of a relaxed emissive state, which has a small polar character and is intrinsically sensitive to the environment.¹²

The TA spectra of RC in *o*-xylene solution [Fig. 4(b)] were found to be similar to the spectra of F8BT exhibiting a SE band below 620 nm and a PA band at longer wavelength. However, compared to the TA spectra of F8BT the SE band showed a dynamic redshift and spectral broadening in the first 22 ps [shown in Fig. 4(b)] before decaying, indicating a stronger nuclear relaxation after photoexcitation.

Figure 2(c) shows the TA spectra of RC in chloroform solution. The SE and PA bands were observed at very early times (hundreds of femtosecond). However, no spectral diffusion could be traced and within 3 ps, the SE band evolved into a broad absorption band, which decayed slowly over the time scale of the experiment. The broad band shows a reduced PA response at 590 nm, which corresponds to the spectral region where the RC PL spectrum in chloroform solution peaks. This is ascribed to the competition between the SE and PA signal of the CT state. Similar spectral features have been observed in the *o*-DCB solution [Fig. 4(d)], although they evolve considerably more slowly. Here, a complete relaxation of the SE band and a redshift to about 590 nm in the first 25 ps have been observed followed by quenching of the SE band and the emergence of a broad absorption band to the infrared.

IV. DISCUSSION

Let us shortly recall the situation in thin films of TFB:F8BT blends spun from chloroform solutions. If excited into the absorption band of F8BT, commonly a SE emission band originating from F8BT is observed at early times, which is then quenched by a very broad PA band. This PA band was ascribed to the generation of polaron pairs at the donor-acceptor interface, more precisely, holes on TFB and electrons on F8BT chains. Once formed, the still-correlated geminate pair is long lived, decaying on typically 40 ns principally forming a triplet exciton.¹³ The broad PA band, which could be detected in the polar solutions of RC has a similar spectral shape to that in F8BT:TFB blend systems, especially in the *o*-DCB solution. However, monitoring the evolution of the PA band on a longer time scale (nanosecond-microsecond) using an extended electronic delay between pump and probe showed a monoexponential decay with a lifetime of (2.5 ± 0.4) , (5.1 ± 0.4) , and (5.9 ± 0.3) ns for the RC in *o*-xylene, chloroform, and *o*-DCB solution very similar to the fluorescence lifetime of the CT state (Fig. 5).

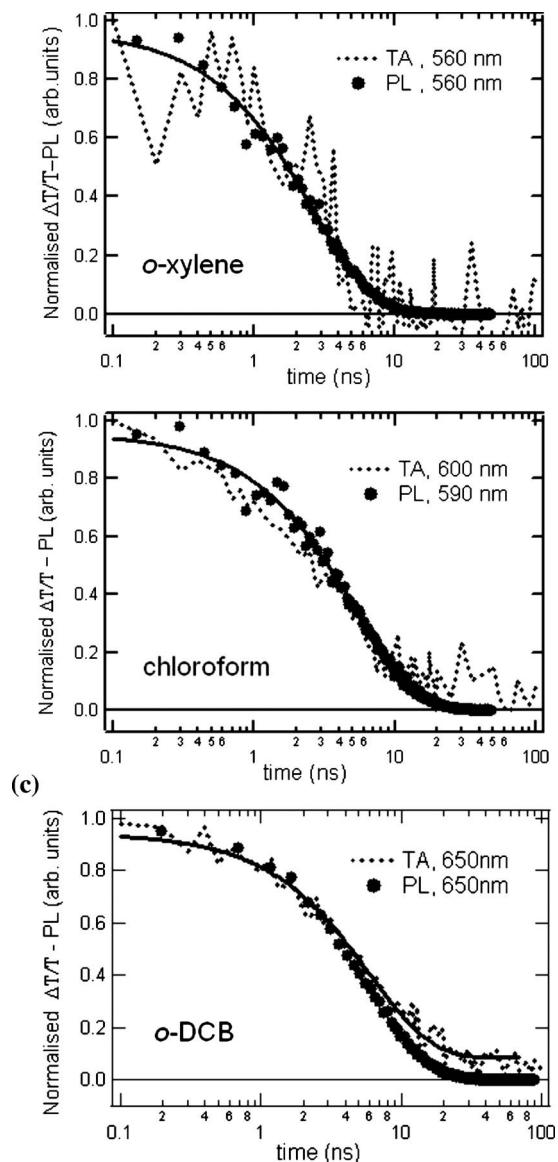


FIG. 5. Normalized transient-absorption kinetics of RC (a) *o*-xylene, (b) chloroform, and (c) *o*-DCB solutions at 560 nm, 600 nm, and 650 nm, respectively, in a time window between 1 ns and 100 μ s. The TA kinetics have been compared with the time-resolved fluorescence lifetime taken from the same solutions at the peak of the PL spectra (filled circles). The experimental data have been fitted (solid line) by a monoexponential function.

Therefore, we rule out the presence of interchain polaron species characterized by a longer lifetime; this assessment is also corroborated by the extremely low concentration of the solution (10^{-7} M) and no evident concentration dependence of the phenomenon. Hence, we assign the broad PA band to the absorption of an intrachain emissive CT state, which carries the same spectral signature as the interchain CT state.

The coulombically bound singlet exciton is the primary photoexcitation in conjugated polymers and charge generation has been attributed to secondary effects.^{14,15} Destabilization of the neutral exciton in favor of charge generation is typically induced in donor-acceptor polymer-polymer blends,¹⁶ where the heterojunction between the two materials

with offset HOMO and LUMO energy levels is the origin of the formation of geminate electron-hole pairs. On the other hand, in small molecular donor-acceptor systems, strongly polar states can be easily induced and intramolecular CT states have been widely studied due to the localized character of the excitations, which enhances the single-molecule character.^{2,17} We emphasize that in the present work, we have observed the evolution of the nature of the primary photoexcitation within the same polymer chain from an excitonic species (Frenkel-type exciton) to an emissive CT state, which has similar absorption characteristics to those of fully separated charges. This has important considerations for potential lasing applications of conjugated polymers. Polaron absorption is an acknowledged problem for light amplification and lasing because of its overlap with the region of maximum gain, which is detrimental for the stimulated emission.¹⁸ However, this study demonstrates a significant blueshift of the PA band of the singlet excited states as it evolves from a neutral exciton to an emissive CT state. Thus, the presence of any excited state with CT character may already be a serious limiting factor for the gain, even in the absence of free polarons, which has severe consequences for the application of this class of materials in organic lasing. On the other hand, the possibility to switch the charge-transfer character of the excited state by changing the polarity of its surrounding may allow for more efficient charge generation in organic solar cells by tuning the dielectric constant of the organic material.

Let us now turn to the origin of the fluorescence shoulder exhibited by the *o*-DCB RC solution around 590 nm. In Fig. 6(a), the PL decay traces probed at different spectral positions are shown. The shoulder was found to evolve with an initial fast component, which is within the time resolution of our instrument, and a long-lived tail resembling the decay of the main peak. The fast decay component is assigned to the charge-transfer process after the selective excitation of F8BT-rich regions on the chain. The origin of the long-lived component is of greater interest and temperature-dependent measurements of the cw-photoluminescence spectrum and of the emission decays have been performed in order to disentangle the dynamics of the two states. Figure 6(b) presents the PL spectra in a temperature range from 281 to 360 K normalized to the maximum of the CT emission band. With increasing temperature, the relative intensity of the high-energy “shoulder” successively increased, becoming dominant above 316 K and closer to the spectral shape of the F8BT. Figure 3(b) presents the normalized PL decays traced at 550 nm at temperatures up to 360 K. The spectral range probed is chosen in a way which reduces the probability of directly probing the emissive CT state whose PL spectrum peaks at 650 nm. The amplitude of the long-lived component progressively increased with increasing temperature. At 316 K, the decay has become entirely monoexponential exhibiting the same lifetime as the CT emission (5.7 ns). It appears that the system underwent a thermally activated backtransfer process from the emissive CT state to the relaxed F8BT exciton from where the fluorescence of the blue edge of the spectrum arises. It is worth mentioning that the fluorescence spectrum of F8BT in *o*-DCB solution did not show any temperature dependence. The inset in Fig. 3(b) shows an Arrhen-

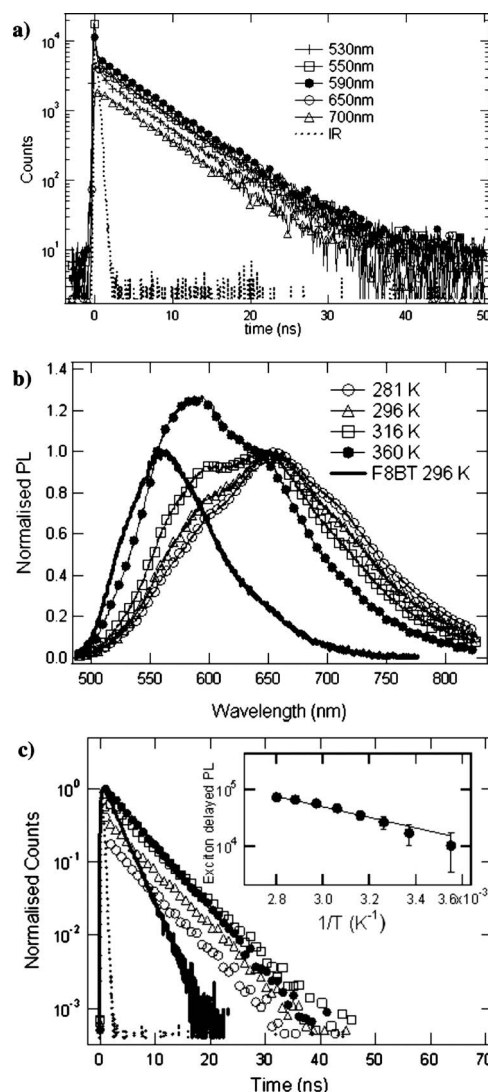


FIG. 6. (a) Time-resolved PL decays transients of *o*-DCB diluted solution traced at different spectral positions. Decays measured at room temperature. The instrument response is also shown. (b) Temperature-dependent PL spectra of RC in *o*-DCB diluted solution, normalized at 650 nm. The PL spectrum of F8BT *o*-DCB diluted solution is also shown. (c) Time-resolved PL decay transients at different temperatures traced at 550 nm of the same solution. The time-resolved PL decay of F8BT *o*-DCB solution and the instrument response are also shown. Excitation at 470 nm. The inset shows the PL intensity dependence on temperature for the short-wavelength part of the spectrum of RC *o*-DCB solution, obtained by integrating the decay traces between 10 and 40 ns. The straight line corresponds to a Boltzmann-type fit.

ius plot of the intensity of fluorescence originating from the F8BT units, which was obtained by integrating the PL decays from about 10 to 40 ns. In this time range, the emission from excited F8BT singlet states originates exclusively from the electron backtransfer process. We found the activation energy of about (190 ± 30) meV for the backtransfer process from the CT state to the excitonic state of the F8BT units with an attempt frequency on the order of 10^8 Hz. We consider this energy as the total free-energy difference between the two states comprising the differences in configuration,

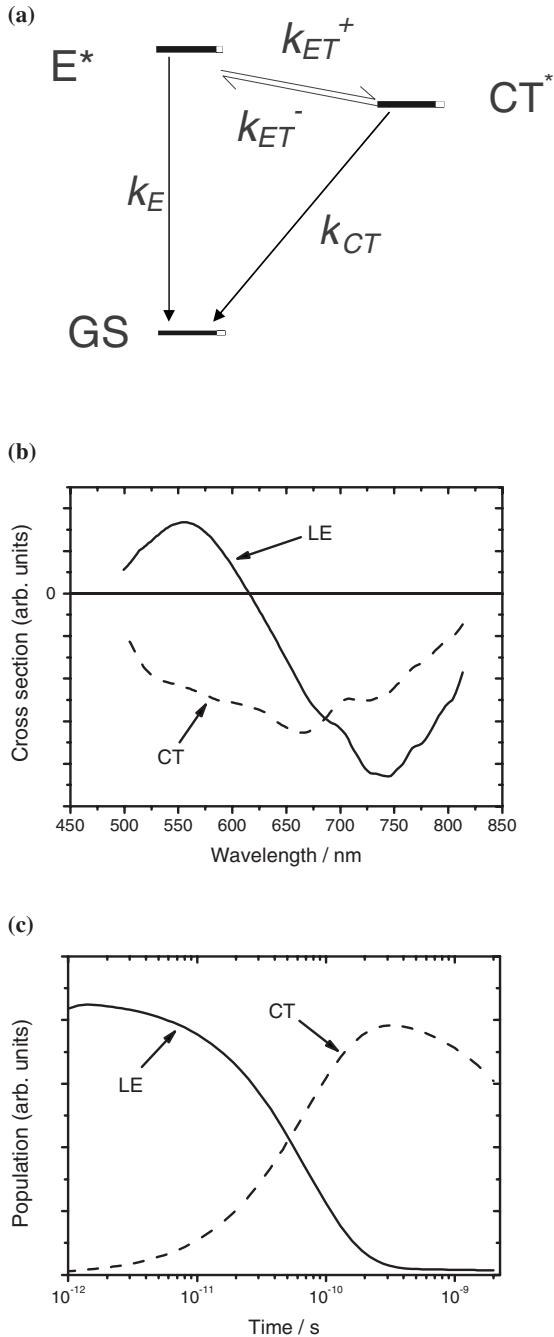


FIG. 7. (a) Charge-transfer model rationalized by the rate Eqs. (2) and (3). (b) The spectral profiles of the locally excited (LE) and the CT state of the random copolymer in *o*-DCB solution obtained from globally fitting the transient-absorption data. (c) Population dynamics of the LE and the CT state of the random copolymer in *o*-DCB solution obtained from a global fit of the transient-absorption data set.

dielectric screening, and rearranged electronic state. The charge-transfer processes have been modeled using rate equations which take into account the forward and backward charge transfer between the Frenkel exciton (E^*) and the CT state [Fig. 7(a)],

$$\frac{d[E^*]}{dt} = k_{ET^-}[CT^*] - (k_E + k_{ET^+})[E^*],$$

$$\frac{d[CT^*]}{dt} = k_{ET^+}[E^*] - (k_{CT} + k_{ET^-})[CT^*],$$

where k_{ET^+} and k_{ET^-} indicate the forward and backward charge-transfer rate while k_E and k_{CT} are the fluorescence rate of the singlet excited state and the CT state.¹⁹ In the chloroform solution, a very fast quenching of the SE band did not allow us to observe any spectral relaxation of the F8BT singlet state since it very rapidly underwent intrachain charge transfer creating the CT state, which later decays with a long lifetime. The backtransfer rate (k_{ET^-}) was found to be much smaller than the forward electron-transfer rate (k_{ET^+}), and therefore neglected when the rate equations were solved. The forward electron-transfer rate of $3.6 \times 10^{11} \text{ s}^{-1}$ was deduced from the fitting of decay transients at 540 nm, where we simultaneously probed the quenching of the F8BT stimulated emission and the emergence of the CT band. In the *o*-DCB solution, further spectral relaxation of the CT state was observed caused by the enhanced polar character of the solvent molecules. The extra solvation of the CT state was also reflected in its longer lifetime, which reduced the coupling to the ground state even further. However, even if it seems to stabilize the CT state further, its generation from the F8BT singlet exciton was slower. We ascribe this delay mainly to slower conformational relaxation dynamics. The conformational relaxation dynamics related to planarization can indeed vary from 10 to 300 ps as the chain length increases.^{20,21} As the spectral shape of the absorption, which resembles the charge absorption feature, indicates, we observed a transition from an exciton-like to a charge-like excited state in the *o*-DCB which involves a strong geometrical rearrangement. It appears that an enhancement of the reorganization energy together with the high viscosity of *o*-DCB is the cause of the slower CT-state formation in *o*-DCB solution compared to chloroform solution. This process was also modeled according to the rate equations described above, however, this time including the competition of the forward and the backward electron transfer. Fitting of the TA kinetics at 570 nm gave a forward electron-transfer rate of $1.8 \times 10^{10} \text{ s}^{-1}$ while the backtransfer rate was found to be $4 \times 10^8 \text{ s}^{-1}$.

A singular value decomposition (SVD) of the TA data sets obtained from chloroform and *o*-DCB solution showed that the data of the former can be sufficiently described by a single component whereas for the latter, the SVD indicated the existence of two components. Further to the SVD analysis, we performed a global fit on the entire matrix of the transient-absorption data from the chloroform and *o*-DCB solution to distinguish the spectral features and the individual dynamics of the neutral excited state and the charge-transfer state and to further verify the rate constants that we obtained from fitting the dynamics at distinct probe energies. For the global fit, the same rate equations that have been described above were used since the photophysical model remains the same. The global fit of the TA data obtained in chloroform solution showed in accordance with the results of the SVD that the entire matrix can be sufficiently described with a single component. It appears that in the chloroform solution, we observe a very fast transition from the neutral

locally excited state to the charge-transfer state which cannot be further resolved in the fitting procedure.

In the *o*-DCB solution, the SVD indicated that the entire data set contains two components. Clearly, the two components can be distinguished from each other by performing a global fit of the entire TA data set using the same rate equations. This time we kept only k_E , i.e., the fluorescence decay rate, fixed, while all other rate constants were left floating. As a result of the global fit, we obtained the individual spectra of the locally excited state and the charge-transfer state as shown in Fig. 7(b).

The spectrum of the neutral exciton exhibits a region of increased transmission peaking at 560 nm and a region of increased absorption beyond 620 nm. The former can be attributed to SE whereas the latter is assigned to PA of the exciton. The spectrum of the second component shows PA over the entire wavelength range and is therefore assigned to the charge-transfer state. It is important to note that the spectral features of the CT state look very similar to the long-time TA spectra obtained from blends of F8BT:TfB in the solid state, where charge transfer takes place between the two intimately mixed components.

Figure 7(c) depicts the individual population dynamics of the locally excited state and the charge-transfer state obtained from the global fit. We obtained a rate constant of $k_{ET}^+ = 1.2 \times 10^{10} \text{ s}^{-1}$ for the forward electron transfer in good agreement with the transfer rate obtained from fitting the individual probe wavelength regions. The rate constant of back electron transfer was determined to $k_{ET}^- = 7.5 \times 10^8 \text{ s}^{-1}$ and the rate constant of charge recombination to $k_{CT} = 1.5 \times 10^8 \text{ s}^{-1}$ both in good agreement with the previous fit and the experimentally observed value for k_{CT} of $1.8 \times 10^8 \text{ s}^{-1}$.

This further supports the validity of the results obtained from the global fit.

In conclusion, we have spectroscopically studied the dielectric-induced switching from a neutral singlet exciton to a charge-transfer state in a donor-acceptor-type random copolymer. In nonpolar solvents, the RC exhibited spectral features typical for localized excited singlet excitons whereas with increasing solvent polarity, a pronounced solvatochromism of the fluorescence accompanied by an increase in the fluorescence lifetime has been observed. The emergence of a broad photoinduced absorption band in the transient-absorption spectra indicated the presence of charge-transfer states. Finally, we have successfully determined the rate constants of the electron-transfer processes by analyzing the dynamics at distinct probe wavelengths and by performing a global fit on the entire TA data set, which also allowed us to approximate the individual TA spectra of the neutral excited state and the charge-transfer state.

ACKNOWLEDGMENTS

A.P. thanks Clare College for funding. F.L. thanks the Deutsche Forschungsgemeinschaft (DFG) for funding and the Clare Hall College, and J.S.K. thanks the ESPRC and the WCU (World Class University) program through the National Research Foundation of Korea funded by the Ministry of Education, Science and Technology (Grant No. R32-10051). We thank Cambridge Display Technology Ltd. for materials supply and EPSRC for financial support. The global fit of the transient absorption data was performed with a MatLab code provided by Larry Lürer from the Politecnico di Milano.

*Corresponding author. ji-seon.kim@imperial.ac.uk

¹A. C. Morteani, P. Sreearunothai, L. M. Herz, R. H. Friend, and C. Silva, *Phys. Rev. Lett.* **92**, 247402 (2004).

²P. F. Barbara, T. J. Meyer, and M. A. Ratner, *J. Chem. Phys.* **100**, 13148 (1996).

³M. Redecker, D. D. C. Bradley, K. J. Baldwin, D. A. Smith, M. Inbasekaran, W. W. Wu, and E. P. Woo, *J. Mater. Chem.* **9**, 2151 (1999).

⁴F. B. Dias, S. King, A. P. Monkman, I. I. Perepichka, M. A. Kryuchkov, I. F. Perepichka, and M. R. Bryce, *J. Phys. Chem. B* **112**, 6557 (2008).

⁵S. I. Hintschich, C. Rothe, S. M. King, S. J. Clark, and A. P. Monkman, *J. Phys. Chem. B* **112**, 16300 (2008).

⁶S. Westenhoff, I. A. Howard, and R. H. Friend, *Phys. Rev. Lett.* **101**, 016102 (2008).

⁷C. Manzoni, D. Polli, and G. Cerullo, *Rev. Sci. Instrum.* **77**, 023103 (2006).

⁸J. S. Kim, L. Lu, P. Sreearunothai, A. Seeley, K.-H. Yim, A. Petrozza, C. E. Murphy, D. Beljonne, J. Cornil, and R. H. Friend, *J. Am. Chem. Soc.* **130**, 13120 (2008).

⁹N. Mataga and T. Kubota, *Molecular Interactions and Electronic Spectra* (Marcel Dekker, New York, 1970).

¹⁰E. E. Neuteboom, S. C. J. Meskers, E. H. A. Beckers, S. Chopin, and R. A. J. Janssen, *J. Phys. Chem. A* **110**, 12363 (2006).

¹¹M. A. Stevens, C. Silva, D. M. Russell, and R. H. Friend, *Phys.*

Rev. B **63**, 165213 (2001).

¹²G. Lanzani, G. Cerullo, S. De Silvestri, G. Barbarella, and G. Sotgiu, *J. Chem. Phys.* **115**, 1623 (2001).

¹³S. Westenhoff, I. A. Howard, J. M. Hodgkiss, K. R. Kirov, H. A. Bronstein, C. K. Williams, N. C. Greenham, and R. H. Friend, *J. Am. Chem. Soc.* **130**, 13653 (2008).

¹⁴V. I. Arkhipov, E. V. Emelianova, and H. Bässler, *Phys. Rev. Lett.* **82**, 1321 (1999).

¹⁵T. Virgili, D. Marinotto, C. Manzoni, G. Cerullo, and G. Lanzani, *Phys. Rev. Lett.* **94**, 117402 (2005).

¹⁶J. J. M. Halls, C. A. Walsh, N. C. Greenham, E. A. Marseglia, R. H. Friend, S. C. Moratti, and A. B. Holmes, *Nature (London)* **376**, 498 (1995).

¹⁷T. Edvinsson, C. Li, N. Pschirer, J. Schöneboom, F. Eickemeyer, R. Sens, G. Boschloo, A. Herrmann, K. Müllen, and A. Hagfeldt, *J. Phys. Chem. C* **111**, 15137 (2007).

¹⁸N. Tessler, *Adv. Mater.* **11**, 363 (1999).

¹⁹J. B. Birks, *Photophysics of Aromatic Molecules* (Wiley, New York, 1970).

²⁰S. I. Hintschich, F. B. Dias, and A. P. Monkman, *Phys. Rev. B* **74**, 045210 (2006).

²¹S. Westenhoff, W. J. D. Beenken, R. H. Friend, N. C. Greenham, A. Yartsev, and V. Sundström, *Phys. Rev. Lett.* **97**, 166804 (2006).